



Validation of a New Methodology to Determine 3-Dimensional Endograft Apposition, Position, and Expansion in the Aortic Neck After Endovascular Aneurysm Repair

Journal of Endovascular Therapy
 2018, Vol. 25(3) 358–365
 © The Author(s) 2018
 Reprints and permissions:
sagepub.com/journalsPermissions.nav
 DOI: 10.1177/1526602818764413
www.jevt.org


Richte C. L. Schuurmann, PhD^{1,2}, Simon P. Overeem, MSc^{1,2} ,
 Kim van Noort, MSc^{1,2}, Bastiaan A. de Vries², Cornelis H. Slump, PhD³,
 and Jean-Paul P. M. de Vries, MD, PhD¹

Abstract

Purpose: To validate a novel methodology employing regular postoperative computed tomography angiography (CTA) scans to assess essential factors contributing to durable endovascular aneurysm repair (EVAR), including endograft deployment accuracy, neck adaptation to radial forces, and effective apposition of the fabric within the aortic neck. **Methods:** Semiautomatic calculation of the apposition surface between the endograft and the infrarenal aortic neck was validated in vitro by comparing the calculated surfaces over a cylindrical silicon model with known dimensions on CTA reconstructions with various slice thicknesses. Interobserver variabilities were assessed for calculating endograft position, apposition, and expansion in a retrospective series of 24 elective EVAR patients using the repeatability coefficient (RC) and the intraclass correlation coefficient (ICC). The variability of these calculations was compared with variability of neck length and diameter measurements on centerline reconstructions of the preoperative and first postoperative CTA scans. **Results:** In vitro validation showed accurate calculation of apposition, with deviation of 2.8% from the true surface for scans with 1-mm slice thickness. Excellent agreement was achieved for calculation of the endograft dimensions (ICC 0.909 to 0.996). Variability was low for calculation of endograft diameter (RC 2.3 mm), fabric distances (RC 5.2 to 5.7 mm), and shortest apposition length (RC 4.1 mm), which was the same as variability of regular neck diameter (RC 0.9 to 1.1 mm) and length (RC 4.0 to 8.0 mm) measurements. **Conclusion:** This retrospective validation study showed that apposition surfaces between an endograft and the infrarenal neck can be calculated accurately and with low variability. Determination of the (ap)position of the endograft in the aortic neck and detection of subtle changes during follow-up are crucial to determining eventual failure after EVAR.

Keywords

3D imaging, 3D reconstructions, abdominal aortic aneurysm, aneurysm neck, endograft, endovascular aneurysm repair, geometry, stent-graft

Introduction

Endovascular aneurysm repair (EVAR) is the preferred treatment modality to exclude an infrarenal abdominal aortic aneurysm (AAA). During the past decade, the envelope has been pushed toward the treatment of complex aortic anatomy by endovascular means.^{1,2} The major limitation of EVAR is to achieve and maintain sufficient seal and fixation in a challenging aortic neck. Challenging preoperative aortic neck anatomy has been associated with acute and long-term complications, such as type Ia endoleak and endograft migration.^{3–7}

Some aspects of EVAR technical success, such as achieving effective apposition in the entire aortic neck, cannot be

assessed accurately on the completion angiogram. Additionally, acute migration and adaptive neck enlargement due to radial

¹Department of Vascular Surgery, St Antonius Hospital, Nieuwegein, the Netherlands

²Technical Medicine, Faculty of Science and Technology, University of Twente, Enschede, the Netherlands

³MIRA Institute for Biomedical Technology and Technical Medicine, University of Twente, Enschede, the Netherlands

Corresponding Author:

Richte C. L. Schuurmann, Department of Vascular Surgery, St Antonius Hospital, Koekoekslaan 1, PO Box 2500, Nieuwegein, 3430 EM, the Netherlands.

Email: richte.schuurmann@gmail.com

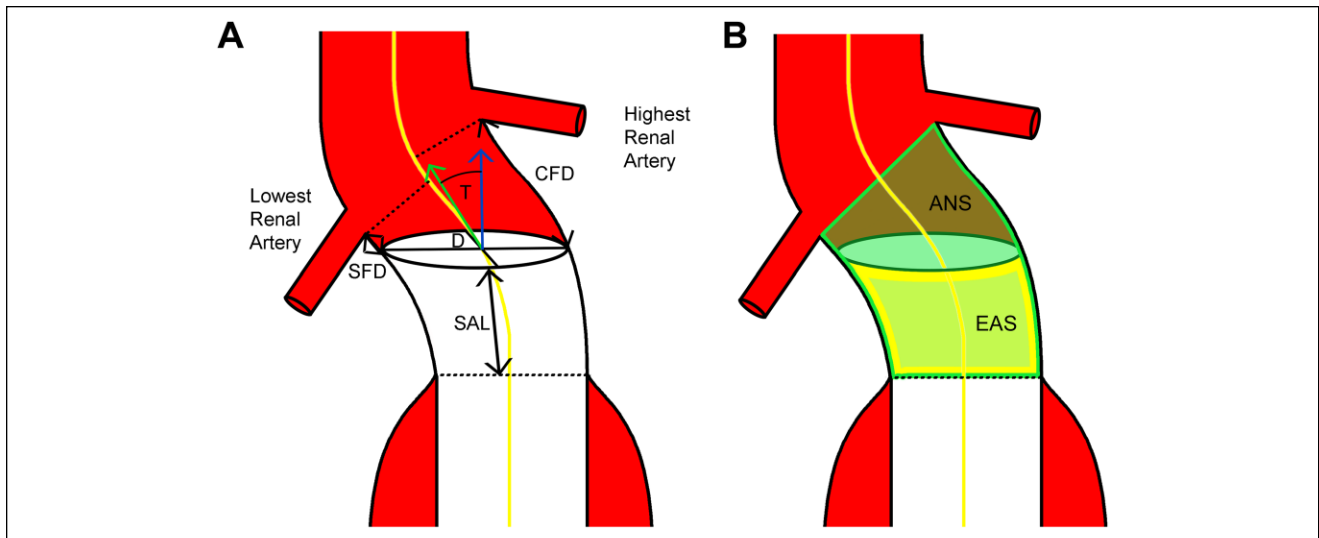


Figure 1. Endograft dimensions describing the 3-dimensional endograft position in the aortic neck. (A) Shortest fabric distance (SFD), shortest distance between the lowest renal artery and the proximal endograft fabric boundary; contralateral fabric distance (CFD), distance between the contralateral renal artery and the proximal fabric boundary; tilt (T), angle between the endograft axis and the aortic neck; endograft fabric diameter (D), average diameter of the proximal end of the main body that is expanded in the aortic neck; and shortest apposition length (SAL), shortest straight-line distance between the proximal circumference of the fabric and the distal end of the aortic neck. (B) Aortic neck surface (ANS), surface area available for sealing in the aortic neck, with a cranial boundary through the distal origins of the renal arteries and a caudal boundary at the distal end of the neck; endograft apposition surface (EAS), actual coverage of the aortic neck by the endograft fabric.

forces are not often adequately evaluated on the first postoperative (1-month) computed tomography angiography (CTA) scan. These 3-dimensional (3D) endograft dimensions within the aortic neck (deployment accuracy, endograft apposition, and endograft expansion at the proximal sealing zone) on the first postoperative CTA scan could serve as a baseline for further follow-up, since changes in these measurements may precede later failure of seal and fixation.

A new methodology has been presented that allows semiautomatic quantification and visualization of the 3D position, apposition, and expansion of the endograft fabric within the aortic neck.⁸ The current study validates the accuracy of these apposition calculations in an *in vitro* study and analyzes their precision in a retrospective series of 24 elective EVAR patients.

Methods

Definitions of Endograft Dimensions

A description of the postoperative endograft dimensions and illustrative examples have been presented previously.⁸ In summary, these dimensions include (1) shortest fabric distance (SFD), the shortest distance between the endograft fabric and the lowest renal artery and the contralateral (CFD) renal artery (Figure 1A); (2) tilt, the angle between the axis of the proximal endograft fabric boundary and the directional vector of the centerline (Figure 1A); (3) endograft expansion, the percentage of the original main body

diameter that is expanded in the aortic neck (the diameter is defined as the average inner diameter over the plane through the proximal edge of the fabric; Figure 1A); and (4) the shortest apposition length (SAL), the shortest distance between the proximal circumference of the fabric and the first slice perpendicular to the centerline where circumferential apposition of the fabric with the aortic neck is lost (Figure 1A). Because of the influence of tilt and complex neck morphology, the lowest part of the proximal fabric boundary is likely the location that is most at risk for seal failure, as represented by (5) the endograft apposition (EAS) surface between the endograft fabric and the aortic wall from the proximal boundary of the fabric to the distal boundary of circumferential apposition (Figure 1B). Aortic neck surface (ANS) is the percentage that has been covered by fabric (Figure 1B).

Calculation of Endograft Dimensions

Dedicated software was developed in Matlab 2016b (The MathWorks, Natick, MA, USA) to calculate the 3D endograft dimensions. The methodology includes 5 steps. First, a centerline was constructed semiautomatically through the aortic lumen on a vascular workstation [3mensio (version 8.1); Pie Medical Imaging BV, Maastricht, the Netherlands] and the following 3D coordinates were identified on the stretched vessel view: (1) the distal edge of the renal artery orifices, (2) the most distal slice perpendicular to the centerline to show circumferential apposition of the fabric with

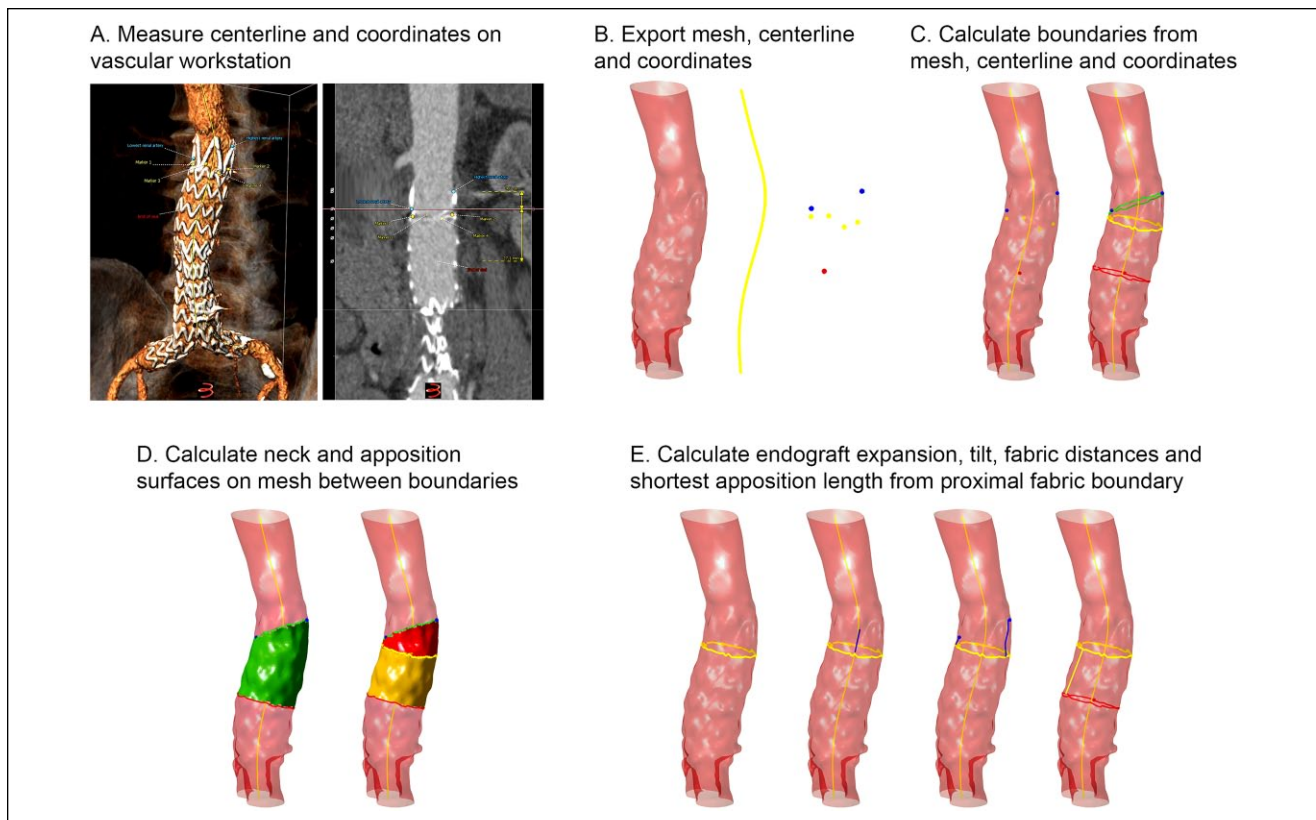


Figure 2. Step-by-step evaluation of the proposed methodology. (A) A centerline is constructed semiautomatically in a vascular workstation, and 3-dimensional coordinates of the renal arteries, proximal end of the fabric, and distal end of the apposition are measured. (B) A mesh of the aortic lumen, the centerline, and the coordinates are exported from the vascular workstation into the dedicated software. (C) Boundaries for the proximal end of the neck (green), proximal end of the fabric (yellow), and distal end of the apposition (red) are constructed. (D) The surface areas between the proximal and distal boundaries are calculated for the aortic neck surface (green) and the endograft apposition surface (yellow). (E) From the proximal end of the fabric, the diameter, tilt relative to the centerline, and fabric distances relative to the renal arteries are calculated.

the aortic neck, and (3) the proximal boundary of the fabric (Figure 2A).

Second, a mesh of the aortic lumen was created by automatic segmentation of the contrast-rich aortic lumen using a tool in 3mensio. Poorly segmented contours, such as low-contrast gaps, bone, small vessels, or chunks of calcium, were manually corrected. Low-intensity thrombus was not segmented. The mesh, centerline, and coordinates were exported into the study software (Figure 2B).

Third, using the mesh, centerline, and 3D coordinates, the software detected boundary circumferences on the mesh of the aortic lumen, defining (1) the proximal end of the aortic neck through the origins of both renal arteries, (2) the proximal edge of the fabric, and (3) the distal end of the full circumferential apposition of the endograft in the aortic neck (Figure 2C). The normal vectors of the proximal and distal boundaries of the aortic neck were obtained from the directional vectors of the centerline.

Fourth, the surfaces were calculated over the aortic mesh between the proximal and distal boundaries of (1) the entire aortic neck and (2) apposition of the fabric with the aortic

neck (Figure 2D). Finally, the following parameters were calculated at the level of the proximal endograft fabric boundary: (1) the average endograft diameter to determine the percentage of expansion of the endograft, (2) the tilt of the axis relative to the direction of the aortic centerline, (3) the shortest and contralateral fabric distances (SFD, CFD) toward the origins of the renal arteries, and (4) the shortest apposition length toward the distal end of circumferential apposition (Figure 2E). The fabric distances were calculated as the Euclidean straight-line distances. For fabric distances >10 mm, distances were recalculated over the curve of the aorta using methods described in detail previously.⁹

Validation of Surface Calculations

The methodology for semiautomatic calculation of surfaces between boundaries over a mesh of the aortic lumen was validated in a silicon cylinder with an inner diameter of 26.8 mm. The cylinder was filled with diluted contrast (Xenetix 300; Guerbet, Sulzbach, Germany) and scanned with the standard local hospital CTA protocol. Images were acquired

on a 256-slice CT scanner (Philips, Best, the Netherlands) using the following parameters: 120-kV tube voltage, 200-mAs tube current time product, 0.75-mm slice spacing, 0.9-mm pitch, and 16×0.75-mm collimation. The true surface of the open cylinder over the length of 30.0 mm was 2529 mm².

The CTA scan with original slice thickness of 0.625 mm was reconstructed into scans with slice thicknesses of 0.67, 0.8, 0.9, 1.0, 1.3, 1.5, 2.0, 2.5, 3.0, 4.0, and 5.0 mm. A mesh of the inner volume of the cylinder was obtained in the 3mensio workstation from each of these CTA scan reconstructions. A centerline was constructed through the center of the cylinder, and coordinate markers were positioned on the cylinder over a distance of 30.0 mm to mark the proximal and distal edges. The mesh surfaces between the upper and lower boundaries were calculated for each of the reconstructions with different slice thicknesses and compared with the true surface of the cylinder.

Variability Analysis

Interobserver variability was analyzed for the endograft dimensions and surface areas calculated from the first postoperative CTA scans of 24 elective EVAR patients (the review of anonymized CT datasets was exempt from institutional review board approval). To provide a baseline for the variability of these calculations, the anatomical neck characteristics (diameter and length) were also measured on the preoperative and first postoperative CTA scans and compared with studies that reported the variability in measuring these neck parameters.^{10–12}

Nine patients were treated with an Endurant endograft (Medtronic, Minneapolis, MN, USA), 9 with a Zenith endograft (Cook, Bloomington, IN, USA), 4 with an Excluder endograft (W.L. Gore & Associates, Flagstaff, AZ, USA), and 2 with an AFX endograft (Endologix, Irvine, CA, USA). No patient had received any additional graft material in the aortic neck (eg, cuffs, bare stents, endoanchors, or parallel grafts).

Two independent, experienced observers performed all centerline constructions, measurements, and mesh exports following the predefined measurement protocol. Each observer was blinded to the results of the other. Neck diameter was defined as the average diameter of the longest and shortest axis measured perpendicular to the centerline from adventitia to adventitia at the level of the distal boundary of the lowest renal artery orifice. In necks with substantial thrombus load, the inner-to-inner neck diameter was measured instead of the outer-to-outer diameter. Neck length was defined as the centerline length from the level of the lowest renal artery baseline to the first slice perpendicular to the centerline where the average aortic diameter increased 10% as compared with the baseline level on preoperative CTA scans. On postoperative CTA scans, the distal end of

the aortic neck was defined by the first slice perpendicular to the centerline that showed interruption of circumferential apposition of the fabric with the aortic neck.

Statistical Analysis

Normality of the data was assessed via visual inspection of the histograms and Q-Q plots. All variables showed a normal distribution, so the data are expressed as means ± standard deviations (SD). The mean difference between paired measurements was calculated, along with the repeatability coefficient (RC), described by Bland and Altman¹³ as 1.96 times the SD of the difference between 2 paired measurements. It is expected that 95% of the differences between the paired measurements are less than the observed RC. Interobserver agreements were calculated with the intraclass correlation coefficient (ICC), which has been tested by absolute agreement in a 2-way mixed model.¹⁴ ICC values >0.8 were considered good agreement. Variability of the calculated endograft diameter and lengths (fabric distances and seal length) were compared to the variability of neck diameter and length measurements using a 3D workstation. Differences between measured and calculated diameters and lengths were assessed with 1-way analysis of variance, with the zero hypothesis of equal variability. The threshold of statistical significance was $p < 0.05$. Statistical analysis was performed with SPSS software (version 23; IBM Corporation, Armonk, NY, USA).

Results

Validation of Surface Calculations

The surface area calculated from the original CTA scan of the silicone model with slice thickness of 0.625 mm was very close to the actual surface (2545 vs 2529 mm²). With increasing slice thickness of the reconstructed CTA scans, the calculated surfaces over the volume segmentation of the cylinder decreased, following a logarithmic pattern (Figure 3). For reconstructions with slice thickness of 1.0 mm, common for CTA scans, the surface was underestimated by 2.8%.

Variability Analysis

The average slice thicknesses of the pre- and postoperative clinical CTA scans were 1.6±0.8 and 1.5±0.8 mm, respectively. The variabilities in measurements of aortic neck morphology and endograft dimensions are shown in Table 1. Excellent agreement was observed for all variables (ICC 0.909 to 0.996).

The variabilities regarding calculation of the endograft dimensions (endograft diameter, fabric distances, shortest apposition length, and endograft apposition surface) were compared with the variabilities in measurement of anatomical

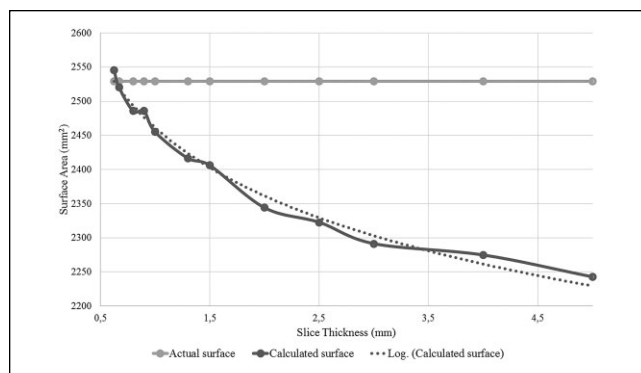


Figure 3. In vitro validation of the surface area calculations on computed tomography angiography (CTA) reconstructions with various slice thicknesses. The calculated surface areas of an open cylinder were compared to the actual surface area. With increasing slice thickness of the reconstructed CTA scan, the calculations underestimate the true surface, following a logarithmic pattern.

neck diameter and length. Both endograft diameter calculations and neck diameter measurements showed very low variability, which was not statistically different ($p=0.054$). The mean differences between observers for these variables were within 1 mm, with 95% of the dispersion within 2 mm. Calculations of fabric distances and shortest apposition length, as well as measurements of neck lengths, also showed low variability. The variabilities of SFD, CFD, and apposition length calculations compared with neck length measurements were not significantly different ($p=0.201$, $p=0.339$, and $p=0.968$, respectively). Mean differences between the observers for these calculations and measurements were within 1 mm, with 95% of the dispersion within 4 to 8 mm.

The average differences between observers for calculation of aortic neck surface and endograft apposition surface were 28 to 43 mm², with an RC of 303 to 692 mm². When this is expressed as the percentage of the mean calculated value, the mean difference is within 2.3% for the surface calculations, compared to 2.6% for the preoperative neck length measurements; 95% of the variability in calculating the surfaces was within 17% to 45%, which was also comparable to measurements of the pre- and postoperative neck lengths (19% to 35%).

Tilt was calculated with a mean interobserver difference of -1.3° and an RC of 9.2° . This parameter could not be compared to any preoperative neck parameter.

Case Example

A 75-year-old man presented with a 72-mm AAA; the proximal neck measured 15 mm long by 23 mm in outer diameter, without thrombus or calcification. The aneurysm was treated with a 28-mm-diameter Talent endoprosthesis oversized by 22% (Figure 4A). The first postoperative CTA scan

showed a reasonably good position of the endograft relative to the renal arteries (SFD 4 mm, CFD 5 mm), with 70% of the aortic neck surface covered, resulting in an apposition length of 12 mm (Figure 4B). The endograft was expanded to 82% of its original diameter. On the second follow-up scan 15 months after the procedure, the endograft had displaced 8 mm caudally compared to the initial position, with an apposition reduction of 10% (Figure 4C). After 27 months, the caudal displacement continued, further reducing the apposition; the endograft was almost fully expanded to 27 mm (Figure 4D). After 51 months, the endograft was fully migrated, resulting in a type Ia endoleak (Figure 4E).

Discussion

A new methodology was validated that enables semiautomatic quantification and visualization of the 3D endograft parameters that are involved in sealing in the infrarenal aortic neck (position, apposition, and expansion) based on regular post-EVAR CTA scans. The in vitro validation showed that the surface calculations were accurate for CTA scans with 0.625- and 1.0-mm slice thicknesses. For increasing slice thickness, the surface is underestimated due to triangulation of the mesh by fewer face triangles. More complex shapes of the aorta may result in larger underestimation of the true surface, but correcting for this error is only relevant when comparing absolute surfaces between scans. The percentage of aortic neck covered by the endograft, which may be more intuitive and important than the absolute surface area, is not affected by this underestimation.

High agreement was found for calculation of the endograft dimensions and measurement of the anatomical neck characteristics. The agreements for measuring neck diameter and length were slightly better than presented in the literature, which may result from the use of a dedicated vascular workstation and a strict measurement protocol.¹⁰⁻¹² Calculation of the endograft dimensions from the mesh of the aortic lumen, centerline, and coordinates was reproducible, with variability margins that were comparable to those of measuring the anatomical neck characteristics on a stretched vessel CTA reconstruction. Variability of tilt calculations could not be compared to the literature since this parameter has not been described previously.

The 3D dimensions of the endograft within the aortic neck should be assessed on the first postoperative CTA scan of every EVAR patient as a quality check of the procedure and to serve as a baseline for further follow-up. Currently, technical success of the procedure is defined as successful deployment of a patent, unobstructed endograft, with secure fixation and absence of type I or III endoleak according to the completion angiogram.¹⁵ These requirements may be achieved, yet deployment of the endograft may be suboptimal, or the neck may not tolerate the expanding endograft.

Table 1. Interobserver Variability for Measuring Aortic Neck Morphology and Endograft Dimensions.^a

	Pre-EVAR					Post-EVAR				
	Mean	MD	RC	ICC	p	Mean	MD	RC	ICC	p
Neck diameter, mm	23.7	0.0	0.9	0.996 (0.991 to 0.998)	<0.001	23.4	-0.1	1.1	0.994 (0.987 to 0.998)	<0.001
Neck length, mm	22.7	0.6	8.0	0.994 (0.986 to 0.997)	<0.001	21.3	-0.3	4.0	0.988 (0.973 to 0.995)	<0.001
Neck surface, mm ²	1532	28	692	0.951 (0.885 to 0.979)	<0.001	1835	43	303	0.988 (0.972 to 0.995)	<0.001
Endograft diameter, mm						23.4	0.4	2.3	0.972 (0.933 to 0.988)	<0.001
Shortest fabric distance, mm						1.8	0.7	5.2	0.906 (0.782 to 0.959)	<0.001
Contralateral fabric distance, mm						10.2	0.5	5.7	0.984 (0.962 to 0.993)	<0.001
Tilt, deg						15.4	-1.3	9.2	0.917 (0.810 to 0.964)	<0.001
Apposition surface, mm ²						1331	-9	307	0.987 (0.971 to 0.995)	<0.001
Shortest apposition length, mm						13.5	-0.2	4.1	0.986 (0.968 to 0.994)	<0.001

Abbreviation: EVAR, endovascular aneurysm repair.

^aData are presented as means, mean difference (MD), repeatability coefficient (RC), and intraclass correlation coefficient (ICC) with 95% confidence interval in parentheses.

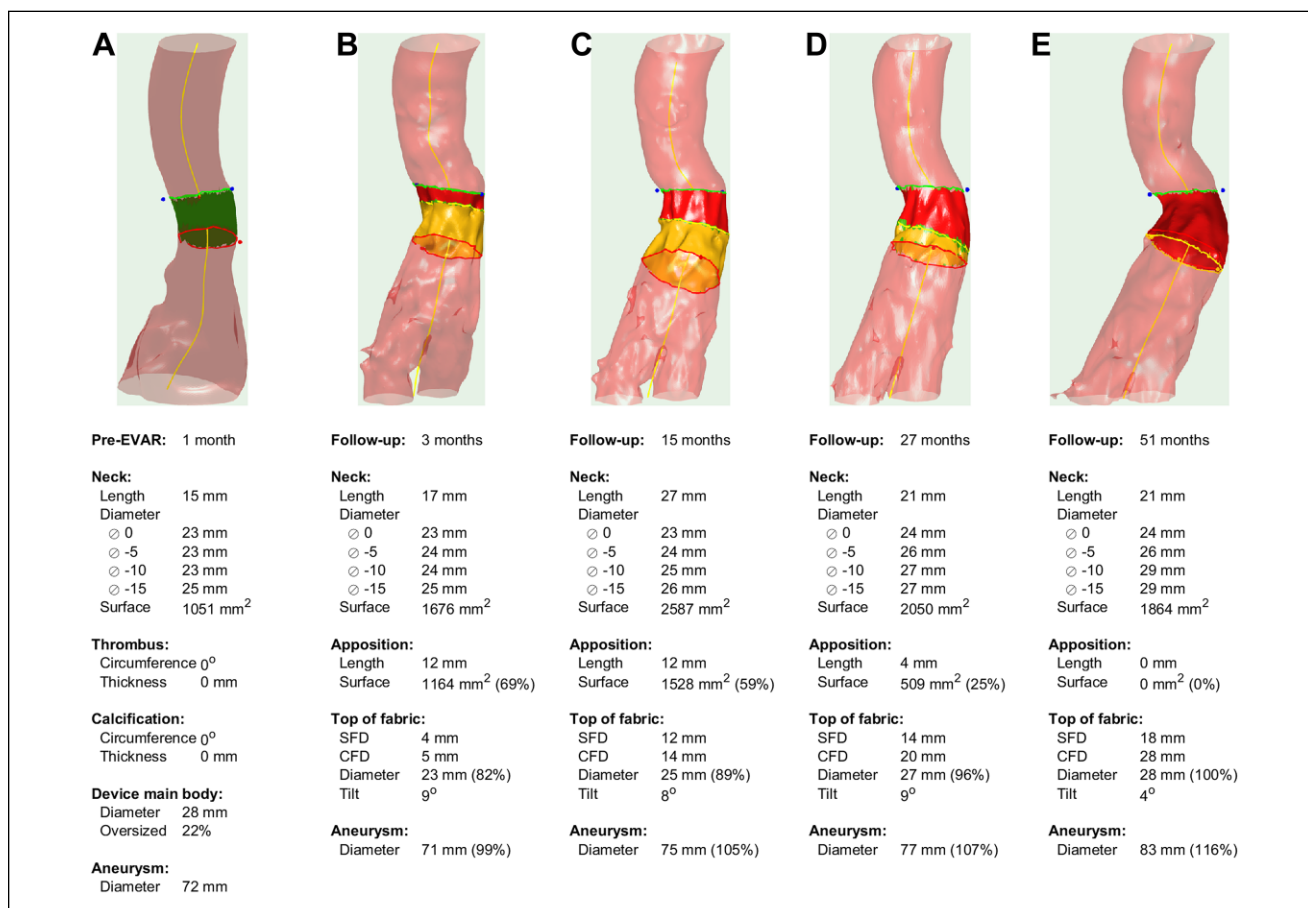


Figure 4. Case example of caudal endograft displacement. (A) Neck morphology on the preoperative computed tomography angiography (CTA) scan showed an unchallenging neck with sufficient oversizing. (B) The first postoperative CTA scan showed reasonably good position, apposition, and expansion of the endograft in the aortic neck. (C to E) Progressive caudal displacement and expansion of the endograft were observed, eventually resulting in loss of apposition and a type Ia endoleak.

Adaptive neck enlargement has recently been described in detail by Tassiopoulos and coworkers,¹⁶ who found >3-mm neck enlargement within 1 month in 12.5% of the patients. With the presented software, neck enlargement can also be appreciated at the level of the proximal edge of the fabric, in addition to measurements in the orthogonal plane at certain distances from the renal artery baseline.

Practice guidelines advise a second CTA scan 1 year after the procedure, which is mainly used to check for endoleaks and obstruction of the endograft.^{17,18} Again, over the course of a year, the actual complication may not have occurred yet, while signs of a progressive process can be detected by analysis of the position, apposition, and expansion of the endograft compared with the first follow-up CTA scan. The effects of radiation and contrast exposure urges physicians to reduce the number of post-EVAR CT scans and replace the 1-year CT scan with duplex ultrasound and radiography. As a result, accurate 3D information on the endograft position and apposition are unavailable during further follow-up. Therefore, accurate analysis of the endograft dimensions on the 1-month CTA scan is essential to identify high-risk patients who may require further CT follow-up.

Time-dependent surface coverage and endograft expansion during the cardiac cycle can be appreciated only with dynamic CT imaging. Four-dimensional (4D) analysis also captures the dynamic properties of different stent designs during the cardiac cycle. The software used in this study was not optimized for 4D analysis, and current analyses were done only on static CTA series, which is a major limitation of this study. However, 4D analysis of endograft dimensions is feasible with the current software by analyzing dynamic scans as a series of 3D volumes, but this is still time consuming. Automatic analysis of dynamic CTA scans is currently a work in progress.

The variability analysis is limited by the retrospective study design. Accuracy and precision of the measurements that are used to calculate the endograft dimensions may vary between observers and with the quality of the CTA scan, which is also the case when measuring regular anatomical characteristics. Accuracy of localizing the proximal fabric edge may also depend on the endograft type. The patients included in this variability analysis were treated with different types of endografts. Endurant, Excluder, and Zenith endografts are equipped with 3 or 4 radiopaque markers that are easily localized in 3D from the reconstructed CTA scan. Devices with 2 or fewer radiopaque markers at the proximal edge of the fabric, such as the Talent or AFX endografts, require localization of the fabric edge based on the stent frame design, which may be more susceptible to error.

Conclusion

A new methodology was validated to quantify and visualize position, apposition, and expansion of the endograft within

the aortic neck after EVAR. Accurate post-EVAR analysis of these endograft dimensions is feasible and reproducible. A large clinical validation study¹⁹ that emphasizes the added value of each of the postoperative endograft dimensions to predict failure of seal and fixation in the proximal neck accompanies the publication of this article.


Declaration of Conflicting Interests

The author(s) declared the following potential conflicts of interest with respect to the research, authorship, and/or publication of this article: Jean-Paul de Vries and Richte Schuurmann are co-founders of the company “Endovascular Diagnostics B.V.,” which holds patent rights over the software used to determine endograft position, expansion, and apposition.

Funding

The author(s) received no financial support for the research, authorship, and/or publication of this article.

ORCID iD

Simon P. Overeem  <https://orcid.org/0000-0002-3282-6654>

References

1. Setacci F, Sirignano P, de Donato G, et al. AAA with a challenging neck: early outcomes using the Endurant stent-graft system. *Eur J Vasc Endovasc Surg.* 2012;44:274–279.
2. Abbruzzese TA, Kwolek CJ, Brewster DC, et al. Outcomes following endovascular abdominal aortic aneurysm repair (EVAR): an anatomic and device-specific analysis. *J Vasc Surg.* 2008;48:19–28.
3. Jordan WD Jr, Ouriel K, Mehta M, et al.; Aneurysm Treatment using the Heli-FX Aortic Securement System Global Registry ANCHOR. Outcome-based anatomic criteria for defining the hostile aortic neck. *J Vasc Surg.* 2015;61:1383–1390.
4. Bastos Gonçalves F, Hoeks SE, Teijink JA, et al. Risk factors for proximal neck complications after endovascular aneurysm repair using the Endurant stentgraft. *Eur J Vasc Endovasc Surg.* 2015;49:156–162.
5. Leurs LJ, Kievit J, Dagnelie PC, et al. Influence of infrarenal neck length on outcome of endovascular abdominal aortic aneurysm repair. *J Endovasc Ther.* 2006;13:640–648.
6. Schuurmann RCL, Ouriel K, Muhs BE, et al. Aortic curvature as a predictor of intraoperative type Ia endoleak. *J Vasc Surg.* 2016;63:596–602.
7. Schuurmann RCL, van Noort K, Overeem SP, et al. Aortic curvature is a predictor of late type Ia endoleak and migration after endovascular aneurysm repair. *J Endovasc Ther.* 2017;24:411–417.
8. Van Noort K, Schuurmann RC, Slump CH, et al. A new method for precise determination of endograft position and apposition in the aortic neck after endovascular aortic aneurysm repair. *J Cardiovasc Surg (Torino).* 2016;57:737–746.
9. Schuurmann RCL, Overeem SP, Ouriel K, et al. A semiautomated method for measuring the 3-dimensional fabric to renal artery distances to determine endograft position after endovascular aneurysm repair. *J Endovasc Ther.* 2017;24:698–706.

10. Ghatwary T, Karthikesalingam A, Patterson B, et al. St George's Vascular Institute Protocol: an accurate and reproducible methodology to enable comprehensive characterization of infrarenal abdominal aortic aneurysm morphology in clinical and research applications. *J Endovasc Ther.* 2012;19:400–414.
11. Ghatwary TM, Patterson BO, Karthikesalingam A, et al. A systematic review of protocols for the three-dimensional morphologic assessment of abdominal aortic aneurysms using computed tomographic angiography. *Cardiovasc Intervent Radiol.* 2013;36:14–24.
12. Kaladji A, Lucas A, Kervio G, et al. Sizing for endovascular aneurysm repair: clinical evaluation of new automated three-dimensional software. *Ann Vasc Surg.* 2010;24:912–920.
13. Bland MJ, Altman DG. Statistical methods for assessing agreement between two methods of clinical measurement. *Lancet.* 1986;327:307–310.
14. Shrout PE, Fleiss JL. Intraclass correlations: Uses in assessing rater reliability. *Psychol Bull.* 1979;86:420–428.
15. Chaikof EL, Blankensteijn JD, Harris PL, et al. Reporting standards for endovascular aortic aneurysm repair. *J Vasc Surg.* 2002;35:1048–1060.
16. Tassiopoulos AK, Monastiriotis S, Jordan WD, et al. Predictors of early aortic neck dilatation after endovascular aneurysm repair with EndoAnchors. *J Vasc Surg.* 2017;66:45–52.
17. Moll FL, Powell JT, Fraedrich G, et al. Management of abdominal aortic aneurysms clinical practice guidelines of the European Society for Vascular Surgery. *Eur J Vasc Endovasc Surg.* 2011;41(Suppl 1):S1–S58.
18. Chaikof EL, Brewster DC, Dalman RL, et al. The care of patients with an abdominal aortic aneurysm: the Society for Vascular Surgery practice guidelines. *J Vasc Surg.* 2009;50(4 Suppl):S2–S49.
19. Schuurmann RCL, Van Noort K, Overeem SP, et al. Determination of endograft apposition, position, and expansion in the aortic neck predicts type Ia endoleak and migration after endovascular aneurysm repair. *J Endovasc Ther.* 2018;25:366–375.